



Studies of the Joining-Relevant Interfacial Properties in the Si-Ti/C and Si-Ti/SiC Systems

Donatella Giuranno , Natalia Sobczak, Grzegorz Bruzda, Rafal Nowak, Wojciech Polkowski, Adelajda Polkowska, Artur Kudyba, and Rada Novakovic

(Submitted October 25, 2019; in revised form January 30, 2020; published online February 13, 2020)

Reactive melt infiltration of Si-based alloys into C preforms and SiC/C composites may be an affordable alternative route to fabricate highly performant lightweighting metal matrix and ceramic matrix composites (CMCs), as well as to obtain reliable and long-term stable joints. In order to optimize reactive infiltration process and to tailor the joint microstructures, the knowledge of interfacial phenomena including thermodynamics, kinetics and surface properties of involved phases (i.e., metals and ceramics) as well as wettability and reactivity occurring between dissimilar materials is of crucial importance. In the present work, the feasibility study of a novel brazing method using Si-Ti alloys as filler for SiC_f/SiC is reported and supported by the analysis of microstructural evolution and interfacial phenomena observed during the joining process. Namely, the CMC joining was successfully obtained via the reactive infiltration approach. The results obtained were critically discussed and compared with the know-how coming from the previously carried out investigations on the wetting and reactivity of Si-Ti melts in contact with glassy-C and HIP-SiC substrates. In particular, the microstructural evolution of the Si-Ti/C and Si-Ti/SiC interfaces during wetting tests and at the joint of CMC parts was analyzed and related to the operating conditions.

Keywords aerospace, automotive and transportation, brazing, ceramics matrix, composites, intermetallic, joining

1. Introduction

Lightweight metal and ceramic matrix composites (MMCs and CMCs) reinforced by high-strength continuous ceramic fibers emerge as ideal structural materials in several applications mainly related to automotive, aircraft and aerospace industries because of their superior high-temperature strength, low density and improved damage tolerance (Ref 1). Both their lower specific weight and improved high-temperature stability

This article is an invited submission to JMEP selected from presentations at the Symposium “Joining and Related Technologies,” belonging to the topic “Processing” at the European Congress and Exhibition on Advanced Materials and Processes (EUROMAT 2019), held September 1-5, 2019, in Stockholm, Sweden, and has been expanded from the original presentation.

Donatella Giuranno, National Research Council of Italy-Institute of Condensed Matter Chemistry and Technologies for Energy, Via De Marini 6, 16149 Genoa, Italy; and **Lukasiewicz Research Network-Foundry Research Institute, Zakopiańska 73 Str., 30-418 Kraków, Poland**; **Natalia Sobczak**, **Grzegorz Bruzda**, **Rafal Nowak**, **Wojciech Polkowski**, **Adelajda Polkowska**, and **Artur Kudyba**, **Lukasiewicz Research Network-Foundry Research Institute, Zakopiańska 73 Str., 30-418 Kraków, Poland**; and **Rada Novakovic**, National Research Council of Italy-Institute of Condensed Matter Chemistry and Technologies for Energy, Via De Marini 6, 16149 Genoa, Italy. Contact e-mails: donatella.giuranno@ge.icmate.cnr.it, natalia.sobczak@iod.krakow.pl, grzegorz.bruzda@iod.krakow.pl, rafal.nowak@iod.krakow.pl, wojciech.polkowski@iod.krakow.pl, adelajda.polkowska@iod.krakow.pl, artur.kudyba@iod.krakow.pl, and rada.novakovic@ge.icmate.cnr.it.

combined with a better corrosion resistance of composites in comparison with monolithic metallic materials used over the past decades enable to make marketable energy-saving technologies capable to decrease the pollutants emissions. Indeed, in the case of MMCs, by combining lightweight materials such as Al-, Si-, Mg- or Ti-based alloys with high stiffness and high specific strength of carbon fibers, ceramic filaments or even dispersed particulates, it is possible to fabricate advanced materials with improved hardness, tensile strength, elastic modulus and other mechanical properties (Ref 2-5). Few other properties, such as electrical and thermal conductivities, coefficient of thermal expansion, coefficient of friction, wear, corrosion and fatigue resistances, can also be addressed by a proper selection of the metal phase according to a specific application (Ref 6). However, the higher temperature capability makes CMCs more versatile as compared to MMCs in lightweight applications (Ref 7).

Today, the most extensively studied CMCs are fiber-reinforced SiC matrix composites, namely C_f/SiC, SiC_f/SiC and C/C-SiC composites. Despite the manufacturing processes of CMCs have reached a high level of reproducibility, their use is currently limited to a great extent by the difficulties encountered in producing successfully large and complex CMCs shapes, and by their assembling and integration with dissimilar materials, i.e., metals, ceramics or other composites.

Reliable joining of the CMC to a metal phase is essential for preserving the overall composite properties and for saving weight of the overall structure. The joint reliability is ensured by the appropriate joint microstructure resulting from the interaction phenomena occurring at the metal/ceramic interfaces.

Among the techniques used for CMCs joining, the most user-friendly include mechanical joining (i.e., rivets) and adhesives, diffusion bonding, transient liquid phase bonding (solid state processes) and brazing (liquid-assisted process). Mechanical joining and adhesives are suitable only for low-

temperature applications. Contrarily, for high-temperature applications, where high strength and corrosion resistance are the key requirements, the active metal brazing is more appropriate (Ref 8).

In general, aiming to preserve the starting SiC matrix thermo-mechanical properties in SiC-based composites, key requirements for a suitable joining technique include the chemical and physical compatibility with the SiC substrate (wettability, thermal expansion, weak SiC dissolution) and joining temperature below 1400 °C in order to avoid fiber degradation in the composites.

As reviewed by Liu et al. (Ref 8), a pressure-less process was developed to join SiC_f/SiC using carbonaceous mixtures as interlayers with a second step consisting of liquid Si infiltration by reaction forming/bonding mechanisms. In this context, several examples are reported in the literature on the use of Si-based alloys as brazing filler materials for promoting successfully joining processes of C_f/SiC and SiC_f/SiC composites by means of interaction mechanisms that control the manufacturing of tailored MMCs and CMCs via capillary and reactive melt infiltration (Ref 9-12).

In this work, an improved joining technique of SiC-based materials by a one-step Si-based alloy infiltration reaction bonding is reported. As documented in Ref 9-11, this method is suitable to produce joints with strong interfacial bonding. Moreover, compared with other joining methods, the reactive infiltration has the advantages to obtain cost-less nearly net shaped joints by reducing processing time and without applying any external pressure.

The feasibility study on a novel Si-16.2Ti (in at.%) eutectic alloy (hereafter indicated as Si-Ti eutectic alloy) used as a filler and the application of the above-mentioned joining/brazing technique to SiC_f/SiC at $T = 1350$ °C under a vacuum was carried out. Both the constituents exhibit excellent overall mechanical and physical properties, such as low density, high-temperature oxidation resistance (due to the growth of a stable passivating and self-healing SiO₂ scale layer) and radiation resistance, making such assembling very promising in most advanced application fields involving aerospace, aviation, military and nuclear power (Ref 12-14). In the latter case, the SiC_f/SiC composites are attracting as structural materials for fusion reactors because of their good mechanical properties at high temperature, low chemical sputtering, high oxygen gettering and very low activation at short and medium terms. Additionally, both Ti and Si elements and their alloys (Ref 15, 16) show very low equilibrium contact angles in short brazing time indicating perfect wetting and adherence to SiC. Few previous attempts to use Si-rich Si-Ti alloys as brazing materials are available in the literature. Indeed, the use of Si-Ti eutectic alloy to join monolithic SiC and SiC_f/SiC at the alloy melting temperature was reported in Ref 12. The rather low process temperature [$T_m = 1330$ °C (Ref 17)] prevented any degradation of the fiber/matrix interfaces in the composite materials. Moreover, all the joints produced did not show any defects and debonding at the interface. In addition, the joint layer appeared well adherent to both the matrix and the fiber interphase, and the brazing alloy infiltration was successfully controlled. In addition, from room temperature to about 600 °C, the joints of SiC_f/SiC composites exhibit the same value of shear strength of 71 ± 10 MPa. However, the

observed joint microstructure consists of two phases of TiSi₂ + Si and, due to the lower melting temperature of Si [$T_m = 1414$ °C (Ref 17)], the nominal temperature of use in service is decreased.

Reliable C_f/C joints have been successfully obtained by a novel two-step brazing method (Ref 11) using Si-Ti eutectic alloy. In particular, effects of the infiltration and brazing operating parameters on the phases formed and resulting mechanical properties of the joints were investigated. The authors were mainly focused to produce Si-TiSi₂-type microstructure in the brazing seam by controlling the process parameters. A SiC phase was detected at the interface between Si-Ti alloy and C_f/C composites resulting in a CTE gradient bonding structure.

Dadras et al. (Ref 18) brazed C_f/C composites by using directly TiSi₂ as filler alloy. The joint obtained showed a maximum shear strength of 34.4 MPa at $T = 1164$ °C, suggesting the use of TiSi₂ braze for applications at high temperatures. However, the lower melting point and better fluidity of Si-Ti eutectic alloy with respect to Ti silicide make it appropriate for the joining at lower temperature, with a good adhesion and limited SiC dissolution. Furthermore, the reduced operating temperature of the process allows better controlling the microstructure evolution and joint stability as compared to the infiltration process of Si-Ti melts into the SiC_f/SiC composites.

Preliminary investigations of thermophysical properties of the liquid phase, solid phase and the interfacial phenomena occurring between the liquid Si-based alloys in contact with C and SiC, in terms of wettability and reactivity (Ref 19-23), are required in order to design liquid-assisted processes such as active brazing and reactive infiltration. Accordingly, to properly design the SiC_f/SiC joining by using liquid Si-Ti eutectics as braze material, the experimental studies on the interfacial properties of Si-16.2Ti/GC (Ref 24) and Si-16.2Ti/SiC (Ref 25) systems were performed as a function of temperature.

An overview of the results in terms of wettability, spreading kinetics and developed interfaces is given in the present work. The wettability studies provided evidences useful in properly addressing the CMC assembly and joining mainly by selecting the suitable process parameters.

The quality of the assembly has been evaluated through metallographic examinations on polished sections by optical microscopy and SEM/EDS techniques both on the whole assembly and at the joint interfaces developed between Si-Ti alloy, SiC matrix and SiC fibers.

2. Experimental Details

2.1 Materials and Sample Preparation

Glassy carbon (GC) provided by Alfa-Aesar® and (hot pressed) HP-SiC by Goodfellow® as substrate materials for wetting experiments with a starting surface roughness value of $R_a \approx 20$ nm and 1 μm, respectively, were selected.

Keraman SiC_f/SiC composites supplied by MT Aerospace, Germany, were used for CMC joining experiments. As detailed in Ref 26, the SiC fibers are Tyranno-S grade 1.6 K (Ube

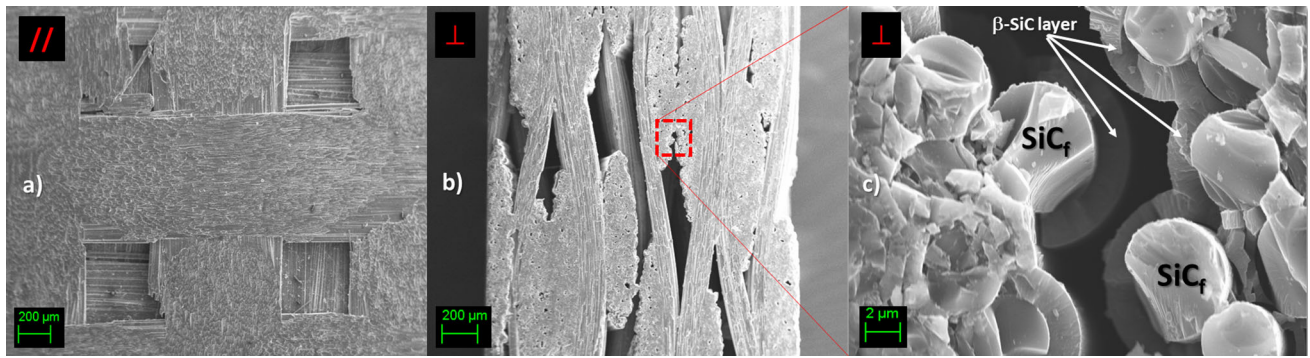


Fig. 1 SEM images of Keraman SiC_f/SiC composite at different magnifications and orientations: parallel (a) and perpendicular (b, c) to the 2D SiC-textured SiC fibers

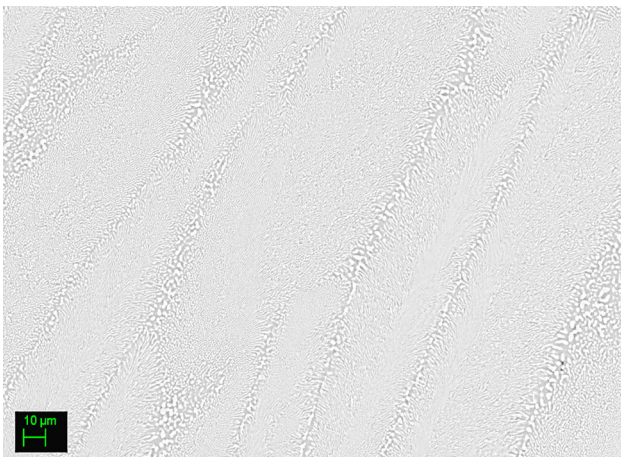


Fig. 2 BSE image of the cross-sectioned Si-Ti eutectic alloy sample as produced by arc melting

Industries, Tokyo, Japan) coated by a thin C layer. All sides are coated with a protective CVD β-SiC layer with a final nominal density of $2.4 \pm 0.05 \text{ g/cm}^3$. Morphological details of the Keraman samples are shown in Fig. 1. As it is observed, SiC matrix, pores and SiC fibers with parallel and perpendicular orientation to the surface are well distinguished (Fig. 1b and c).

For joining experiments, the CMC samples were cut orthogonally to the plies of SiC_f/SiC fibers, avoiding the removal of the CVD-SiC coating layer. The coating acts as a protective barrier for the SiC fibers against oxidation under service conditions, and in the present case, even avoiding the direct contact between the SiC fibers and brazing alloy during the joining process.

The Si-16.2Ti alloy samples were prepared by mixing nominal weights of high-purity Si and Ti (99.98%, Goodfellow). To limit the evaporation and oxidation phenomena, the alloy samples were produced by the arc melting technique under a protective atmosphere with reduced oxygen content, as detailed in Ref 24, 25.

At the cross-sectioned produced Si-Ti eutectic samples, the typical eutectic microstructure was detected by SEM/EDX analyses, as shown in Fig. 2.

Prior to the wetting experiments, the alloy samples and substrates were ultrasonically rinsed in ethanol and dried with compressed air.

2.2 Wetting Experiments by the Sessile Drop Method: Devices and Procedure

At room temperature, the assembled Si-Ti eutectics/substrate couple was placed on a graphite sample holder, located at the central part of the heater and leveled at the horizontal plane.

The alloy/substrate couple was heated by an 800 kHz high-frequency generator coupled to a graphite tube, which provides an atmosphere with reduced oxygen content ($\text{PO}_2 < 10^{-8}$ mbar).

In order to avoid evaporation phenomena and material loss, typically occurring during measurements of liquid Si-based alloys (Ref 20, 25), the wetting experiments were performed under a static Ar ($\text{O}_2 < 0.1$ ppm) atmosphere by the contact heating sessile drop method. The procedure applied was detailed in Ref 24.

During the wetting experiments, the process parameters such as temperature, oxygen partial pressure and total pressure as well as the evolution of contact angles over time (recorded at 10 frames/s) were monitored in real time (Ref 27). Each single frame captured by a CCD camera was processed by an image analysis software ad hoc-developed (ASTRAVIEW[®]) (Ref 28) allowing the automatic acquisition of contact angles and drop geometric variables (R -base radius and H -drop height).

As extensively discussed by the authors Ref 24, 25, the presence of a SiO₂ layer on both the alloy and SiC substrate surface most probably affected the initial stage of the spreading kinetics, mainly at the lower temperatures ($T = 1350 \text{ }^\circ\text{C}$) investigated. Accordingly, targeted wetting experiments were performed by the dispensed drop procedure (Ref 25). In this case, the alloy sample was stored into an Al₂O₃ polycrystalline capillary (diameter of 9 mm) and loaded inside the chamber at room temperature. At the testing temperature, the melted alloy was squeezed through a hole (diameter of 1 mm) by a piston and the formed drop was deposited onto the substrate. During the squeezing, native oxide films are mechanically broken and removed and an oxide-free molten surface is exposed to the surrounding experimental environment (Ref 29).

2.3 CMC Joining: Devices and Procedure

Prior to the joining experiment, two SiC_f/SiC plates (5 mm × 5 mm × 2 mm) were metallographically polished and assembled with the alloy sample on a graphite plate used as sample holder (see Fig. 3). The assembly was introduced into the experimental device and, as in the case of wetting experiments, was degassed under a vacuum ($P_{\text{tot}} \leq 10^{-6}$

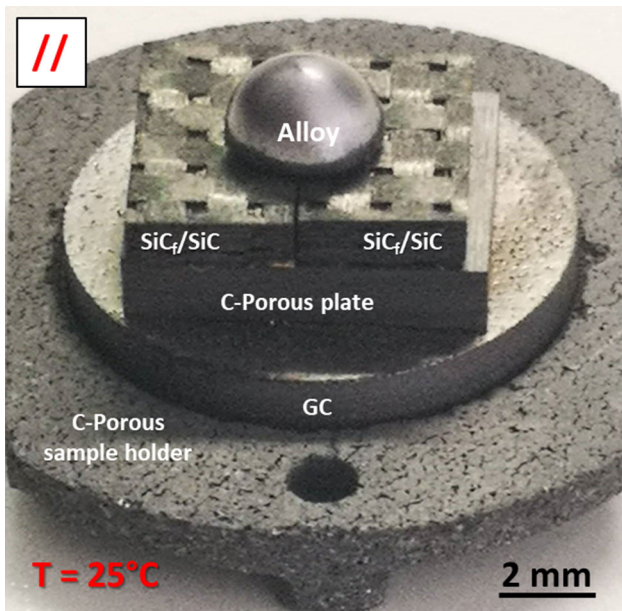


Fig. 3 Si-Ti alloy/CMC couple as assembled during the joining experiments

mbar) for 2 h. Under the same total pressure, the temperature of the sample was raised up to $T = 1350\text{ }^{\circ}\text{C}$ selected as joining temperature. The evolution of the joining process was monitored in real time by a high-resolution CCD camera connected to a computer. The selected temperature was kept constant until the alloy disappearance into the assembly, and then, to preserve the new formed reaction products and developed joint interface microstructure, the sample was quenched (cooling rate $10\text{ }^{\circ}\text{C/s}$) by turning off the power to the heater.

2.4 Surface and Microstructural Characterization

After the wetting and joining tests, all the Si-Ti eutectic alloy/substrate samples were embedded into epoxy resin, cross-sectioned and metallographically polished for the microstructural characterization. In order to analyze the microstructure and reaction products, an optical microscope (ZEISS©) and a scanning electron microscopy (SEM) equipped with an energy-dispersive x-ray detectors (EDS) were used.

3. Results and Discussion

3.1 Wettability by the Sessile Drop Method as a Function of Temperature and Substrate

The wetting kinetics in the liquid Si-Ti eutectic alloy/GC system observed during the early stage of the experiments (upon first 100 s) at three different temperatures are shown in Fig. 4. As expected, Si-Ti eutectics exhibit different spreading behaviors on GC, as well as different spreading rates (U_{spr}) as follows: $U_{\text{spr}}(1350\text{ }^{\circ}\text{C}) < U_{\text{spr}}(1400\text{ }^{\circ}\text{C}) < U_{\text{spr}}(1450\text{ }^{\circ}\text{C})$. Indeed, increasing the temperature, the C dissolution and its reactivity with liquid Si (leading to the SiC formation) are enhanced.

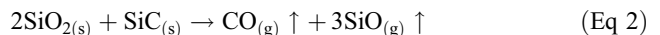
In addition, at higher temperatures, Si evaporation/condensation phenomena are promoted, as reported in Ref 24, 25, as well as the rate of advancing of contact angle up to the achievement of the steady state condition (i.e., final contact angle value). Moreover, the increase in temperature enhances the growth kinetics of SiC at the liquid Si-Ti eutectics/GC interface.

As it is reported in Table 1, the same value of final contact angle was measured at the three different testing temperatures. It may be due to the “pinning” effect of SiC crystals epitaxially grown at the alloy/substrate interface.

The oxide-free wetting behaviors of the liquid Si-Ti eutectics on both GC and SiC substrates at $T = 1450\text{ }^{\circ}\text{C}$ under an Ar atmosphere are shown in Fig. 5. Although the isothermal temperature is $120\text{ }^{\circ}\text{C}$ higher than the melting point of Si-16.2Ti eutectics ($T_m = 1330\text{ }^{\circ}\text{C}$), a delay in the complete melting was observed on both substrates (Ref 17), as widely discussed in Ref 25. It can be due to the presence of a primary SiO_2 layer at the alloy surface. However, the layer of native oxide is decomposed into volatile Si monoxide by the reaction with the underlying Si appearing at the liquid state (Ref 15):



In addition, further delay of 3 s observed during the alloy spreading onto the SiC substrate can be attributed to the higher roughness of the SiC surface ($1\text{ }\mu\text{m}$) with respect to the GC substrate (20 nm) and due to the presence of SiO_2 at the SiC surface which undergoes to decomposition by following reaction (1) when an oxide-free Si surface appears at the interface. As reported in Ref 30, another equilibrium could be taken into account favoring the decomposition of the SiO_2 layer present at the Si-Ti eutectics/SiC interface:



For the above-mentioned reasons, the contact angle values observed just after the alloy melting were not considered for the analysis of the spreading kinetics in both systems, i.e., the Si-16.2Ti/SiC and the Si-16.2Ti/GC at $T = 1350\text{ }^{\circ}\text{C}$.

The advancing of the contact angles during the first 100 s for the Si-16.2Ti/GC and Si-16.2Ti/SiC systems is compared in Fig. 5. In particular, Si-Ti eutectics exhibits different rates of wetting kinetics on GC and SiC substrates. Consequently, $U_{\text{spr}}(\text{GC}) < U_{\text{spr}}(\text{SiC})$ was observed.

The different spreading behavior observed is controlled by wetting for non-reactive systems and by chemical reaction-limited spreading for reactive system, on SiC and GC, respectively (Ref 15). As already introduced, the same equilibrium contact angle value of $\theta \approx 43\text{-}44^{\circ}$ was measured in Si-16.2Ti/GC and Si-16.2Ti/SiC systems as a further confirmation that the real wettable substrate is SiC even in the case of GC as starting substrate. In fact, a double layer of SiC was detected as unique reaction product at Si-Ti eutectics/GC interface obtained at $T = 1450\text{ }^{\circ}\text{C}$, with an average thickness of $5\text{-}7\text{ }\mu\text{m}$, as reported in Ref 24. On the contrary, the absence of reaction layer between Si-Ti eutectics and the SiC substrate was revealed, as an example of non-reactive system (Ref 25). However, a slight erosion of the SiC substrate at the alloy/SiC interface was evidenced.

In both cases, the solidified alloy drop exhibits a Si-TiSi_2 two-phase microstructure. In particular, rounded and needle-shaped TiSi_2 crystals embedded in a Si matrix were detected.

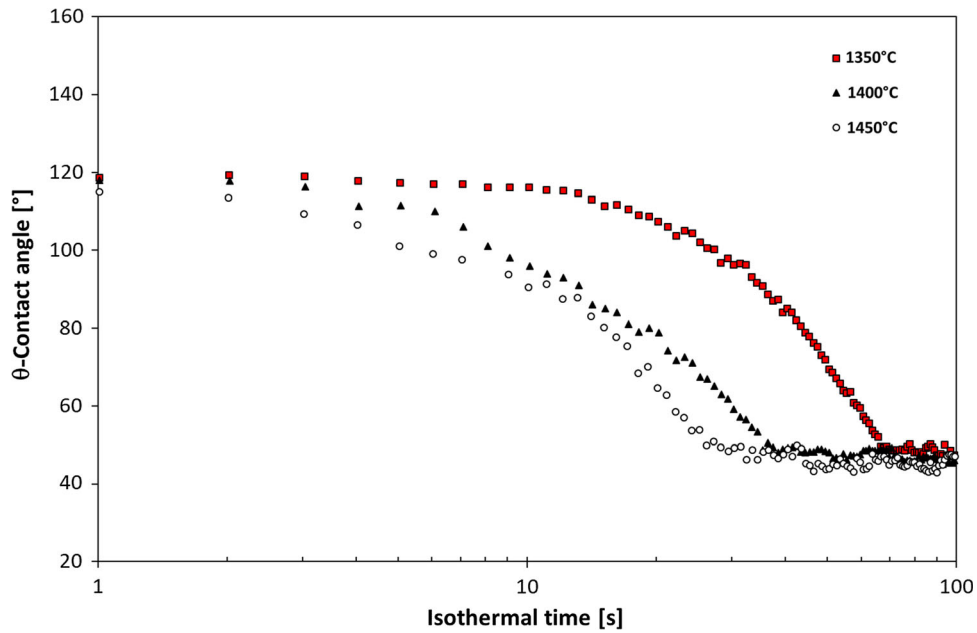


Fig. 4 Wettability of the Si-16.2Ti/GC couples for 15 min under an Ar atmosphere at: (filled square) $T = 1350\text{ }^{\circ}\text{C}$; (filled triangle) $T = 1400\text{ }^{\circ}\text{C}$ and (circle) $T = 1450\text{ }^{\circ}\text{C}$

Table 1 Final contact angle values measured by the sessile drop method at Si-16.2at.%Ti/GC triple lines within the wetting tests performed at $T = 1350, 1400, 1450\text{ }^{\circ}\text{C}$ under an Ar atmosphere after $t = 15\text{ min}$

Alloy/GC	Temperature, $^{\circ}\text{C}$	Contact angle, $t \sim 15\text{ min}$, $^{\circ}$
Si-16.2at.%Ti	1350	44 ± 1
	1400	43 ± 1
	1450	44 ± 2

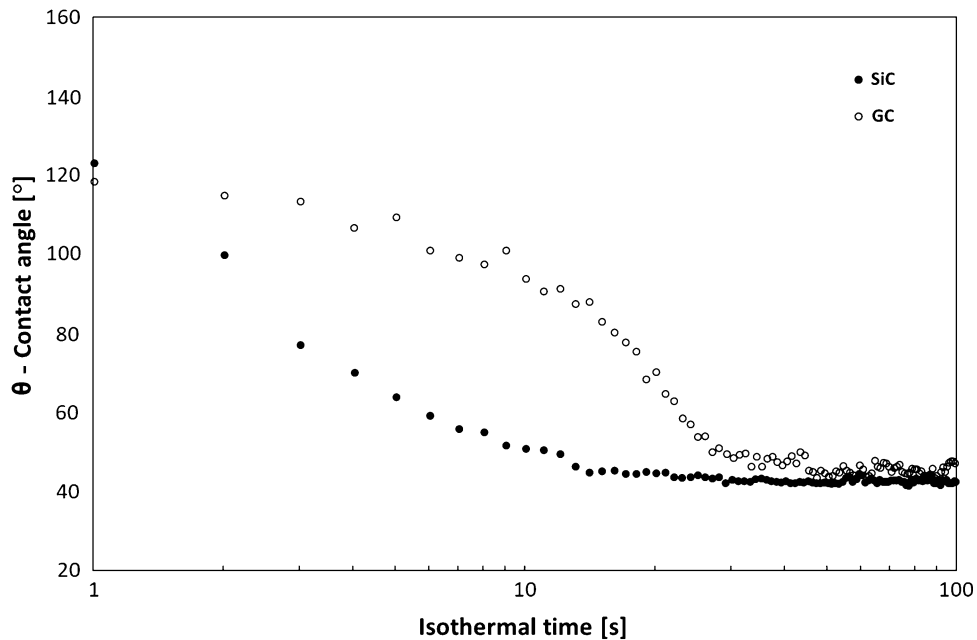


Fig. 5 Contact angle values as a function of time of Si-Ti eutectics/SiC (filled circle) and Si-Ti eutectics/GC (circle) at $T = 1450\text{ }^{\circ}\text{C}$ measured by the sessile drop method under oxide-free conditions

3.2 SiC_r/SiC Composites Joined by Liquid Si-16.2Ti Alloy

The results obtained by wetting tests performed on the Si-16.2Ti/GC couple indicate that the wettability is mainly

controlled by reactive mechanism. Accordingly, both spreading kinetics and interfacial microstructures are dependent on the temperature. Although not yet investigated, the temperature

should be also the key process parameter driving the spreading kinetics at the Si-16.2Ti/SiC triple line, as documented by Drevet and Eustathopoulos Ref 15 for SiC in contact with other Si-based alloys. In addition, competitive phenomena such as the presence of a SiO₂ native oxide layer at the surface of the alloy drop as well as at the SiC surface substrate affect the spreading kinetics within the melting stage, mainly at lower temperatures. On the other hand, the final contact angle values that are constant over long time intervals are not influenced by the temperature even considering the more pronounced evaporation/condensation phenomena observed at higher temperatures.

Clear evidences were obtained that the wettability and in particular the spreading kinetics are controlled by the formation and thickening of SiC at the interface and at the triple line. Such experimental observations are helpful in finding the suitable procedure for joining SiC_f/SiC by Si-16Ti alloy. By taking into account that the capillary infiltration of the liquid alloy between SiC/SiC_f composites will be the main phenomenon occurring during the joining process, the temperature seems to be the key process parameter to retain enough amount of Si-Ti alloy in the joining area.

As reported in Ref 31, it is possible to promote spreading at lower temperatures with respect to those of infiltration and consequently to preserve the joint stability. Considering the presence of SiO₂ as native oxide and its influence on the alloy melting stage, observed at lower temperatures, the CMC joining under a vacuum with reduced oxygen content was performed.

The image sequences of Si-Ti eutectics during the SiC_f/SiC joining process performed at $T = 1350^{\circ}\text{C}$ are shown in Fig. 6. At $t = 0$, two SiC_f/SiC pieces are well distinguished. The distance between the two composites is around 0.01 mm. As shown in Fig. 6(b), it is possible to analyze the joining process

following the evolution of the drop geometrical parameters, specifically the drop base radius (R) and drop height (H). In particular, as soon as the liquid phase appeared in contact with SiC, the alloy started to wet the composites with a coherent increase in the alloy drop radius. However, during this stage, the upper part of the drop is only partially melted ($0 < t < 5$ s), and consequently, a weak change in the height of the drop is revealed. Since the same behavior was observed during the wetting tests performed at $T = 1450^{\circ}\text{C}$, most probably the dissolution of SiO₂ by reactions (1) and (2) is taking place at the interface. Contrarily, at $t > 5$ s a strong decrease in the drop height is observed, while the drop radius substantially does not change until the end of experiment. Such behavior is typical for infiltration mechanisms basically controlled by capillary phenomena (Ref 31).

In addition, as the joining process proceeds, a rough contour of the alloy drop was observed due to the appearance of TiSi₂ as solid phase segregated at the surface because of the reduced Si content inside the melt. Since the absence of evaporation was confirmed by checking the final weight of the sample, the Si consumption is due to its reaction with the residual C still present inside the SiC_f/SiC composite and to the infiltration leading to further consumption of Si into the porous graphite plate located at the bottom of the assembly (see Fig. 7b). In fact, as shown in Fig. 7(c), SiC crystals are detected at the pore walls as products of the reaction between liquid Si and C.

The BSE/SEM analyses performed in the SiC_f/SiC joined area are shown in Fig. 8. As observed during wetting tests, the joint microstructure consists of globular TiSi₂ embedded in pure Si (Fig. 8b). The anisotropic distribution of the TiSi₂ inside Si should increase the overall mechanical response of the joint. Moreover, the Si-Ti alloy perfectly adhered to the SiC_f/SiC surface and a “brush-like” interface, resulting from the SiC

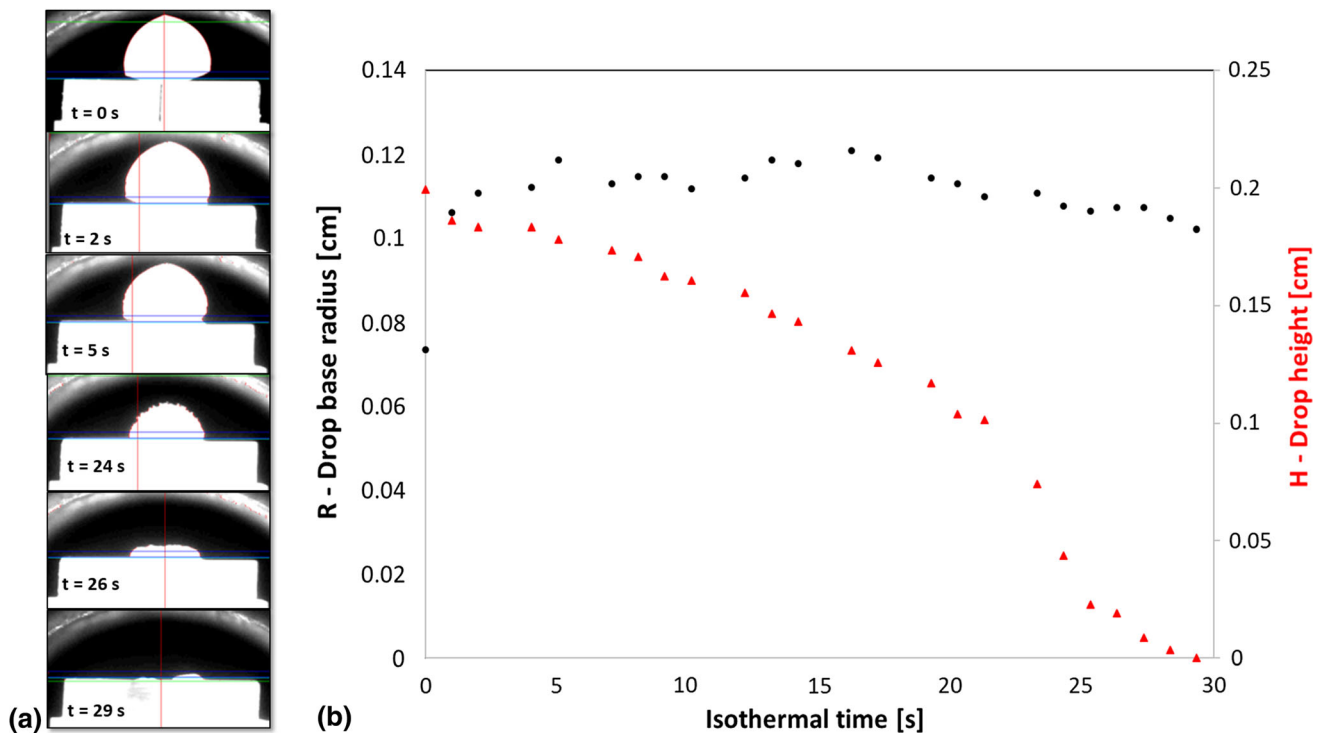


Fig. 6 Si-Ti eutectics on SiC_f/SiC during joining process performed at $T = 1350^{\circ}\text{C}$: (a) time sequence images and (b) isothermal evolution of R -drop base radius and H -drop height over time

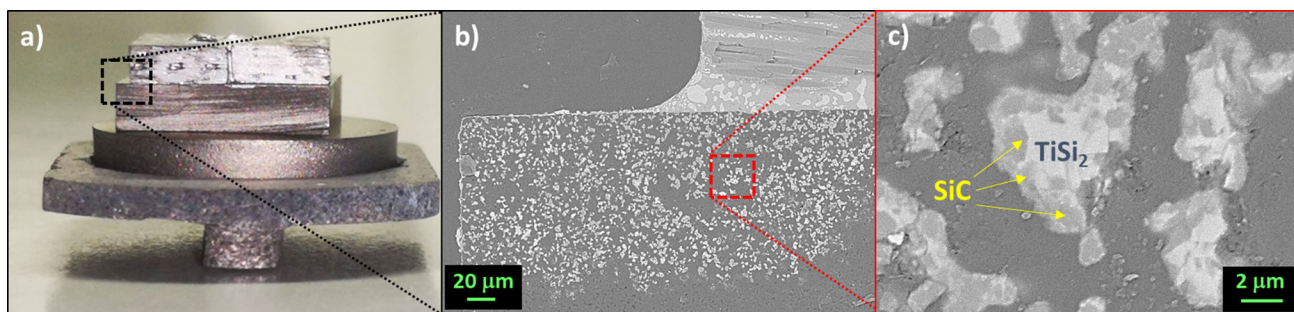


Fig. 7 SiC_f/SiC joined by Si-Ti eutectics at $T = 1350\text{ }^{\circ}\text{C}$: (a) assembly and BSE/EDS analyses performed at the infiltrated area of porous graphite (sample holder)

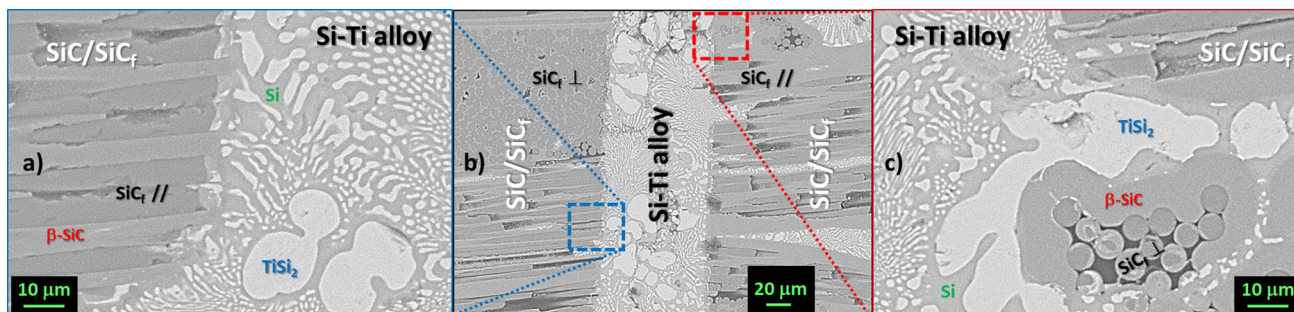


Fig. 8 BSE/EDS analyses performed at the Si-Ti/SiC interfaces obtained at $T = 1350\text{ }^{\circ}\text{C}$: (a) Si-Ti alloy // SiC_f, (b) Si-Ti alloy // \perp SiC_f and (c) Si-Ti alloy / \perp SiC_f interfaces

fibers degradation with a consequent alloy penetration of about $5\text{ }\mu\text{m}$ inside the SiC matrix, were observed (see Fig. 8a).

In particular, the increased joint surface area should enhance the mechanical strength of the joint by increasing the mechanical interlocking. The same phenomenon was observed at the SiC_f/SiC joint produced by using an Ag-Cu-Ti brazing alloy (Ref 26). In that case, in order to obtain engineered surfaces, the SiC_f/SiC was previously thermal treated. Specifically, a selective thermal removal procedure of SiC fibers from SiC_f/SiC composites was applied by heating the composites at $T = 1450\text{ }^{\circ}\text{C}$ for 2 h under an Ar flowing atmosphere. As the authors explained, the SiC_f used as reinforcement consist of an amorphous SiTi_zOxCy phase and β -SiC nanocrystallites. During the heat treatment, these fibers are subjected to a thermal degradation due to the development of gaseous products such as SiO and CO. In the present case, the same phenomenon might be occurred and enhanced by the low total pressure and reduced oxygen content imposed during the joining process. In addition, the SiC dissolution by the liquid Si-Ti alloy, already observed during the wetting experiments, cannot be excluded as concomitant phenomenon. Contrarily, the absence of dissolution/degradation phenomena of the β -SiC coating on the SiC fibers were revealed at least at $T = 1350\text{ }^{\circ}\text{C}$ (see Fig. 8c).

4. Conclusion

The proof of concept in using reactive infiltration process as CMC joining technique with Si-based alloys was successfully realized. Specifically, SiC_f/SiC pieces were effortlessly joined by the liquid Si-16.2at.%Ti alloy at $T = 1350\text{ }^{\circ}\text{C}$ under vacuum

conditions. The know-how previously acquired upon investigations of the interaction phenomena occurred at the Si-16.2at.%Ti/GC and Si-16.2at.%Ti/SiC interfaces was the basis for the optimization of both the joining process and fillers. In particular, the selection of suitable joining process parameters (i.e., temperature, time, atmosphere), the interfacial phenomena observed in terms of wettability, reactivity and microstructural evolution of the interface were carefully analyzed, even in the view of the other Si-Ti alloy compositions to be tested as candidate braze materials. The methodology used in the present work can be also useful for the fabrication of lightweight composites via the reactive infiltration approach.

Acknowledgment

The NCN—National Science Center, Poland, is greatly acknowledged for the financial support through the POLONEZ Project Number UMO-2016/23/P/ST8/01916. This project was carried out under POLONEZ-3 program which has received funding from European Union's Horizon 2020 research and innovation program under Marie Skłodowska-Curie Grant agreement. No. 665778. DG and RN wish to thank Mr Francesco Mocellin for his technical assistance.



Open Access

This article is licensed under a Creative Commons Attribution 4.0 International License, which permits use, sharing, adaptation, distribution and reproduction in any medium or format, as long as you give appropriate credit to the original author(s) and the source, provide a link to the Creative Commons licence, and indicate if changes were made. The images or other third party material in this article are included in the article's Creative Commons licence, unless indicated otherwise in a credit line to the material. If material is not included in the article's Creative Commons licence and your intended use is not permitted by statutory regulation or exceeds the permitted use, you will need to obtain permission directly from the copyright holder. To view a copy of this licence, visit <http://creativecommons.org/licenses/by/4.0/>.

References

1. D.B. Miracle, Aeronautical applications of metal-matrix composites, *ASM Handbook*, S.D. Henry et al., Ed., ASM International, Ohio, 2001,
2. X. Zhang, Y. Chen, and J. Hu, Recent Advances in the Development of Aerospace Materials, *Prog. Aerosp. Sci.*, 2018, **97**, p 22–34
3. H. Singh, S.J. Nrip, and A.K. Tyagi, An Overview of Metal Matrix Composite: Processing and SiC Based Mechanical Properties, *J. Eng. Res. Stud.*, 2011, **2**(4), p 72–78
4. K. Shirvanimoghaddam, S.U. Hamim, M.K. Akbari, S.M. Fakhro-seini, H. Khayyam, A.H. Pakseresht, E. Ghasali, M. Zabet, K.S. Munir, S. Jia, J.P. Davim, and M. Naebe, Carbon Fiber Reinforced Metal Matrix Composites: Fabrication Processes and Properties, *Compos. Part A Appl. Sci. Man.*, 2017, **92**, p 70–96
5. E.P. Simonenko, D.V. Sevastyanov, N.P. Simonenko, V.G. Sevastyanov, and N.T. Kuznetsov, Promising Ultra-High-Temperature Ceramic Materials for Aerospace Applications, *Russ. J. Inorg. Chem.*, 2013, **58**(14), p 1669–1693
6. S.T. Mileiko, Constituent Compatibility and Microstructural Stability, *Compr. Compos. Mater.*, 2000, **4**, p 265–287
7. J. Binner, M. Porter, B. Baker, J. Zou, V. Venkatachalam, V.R. Diaz, A. D'Angio, P. Ramanujam, T. Zhang, and T.S.R.C. Murthy, Selection, Processing, Properties and Applications of Ultra-High Temperature Ceramic Matrix Composites, UHTCMCs—A Review, *Int. Mater. Rev.*, 2019, <https://doi.org/10.1080/09506608.2019.1652006>
8. G. Liu, X. Zhang, J. Yang, and G. Qiao, Recent Advances in Joining of SiC-Based Materials (Monolithic SiC and SiCf/SiC Composites: Joining Processes, Joint Strength, and Interfacial Behavior, *J. Adv. Ceram.*, 2019, **8**(1), p 19–38
9. X. Wua, B. Peia, Y. Zhua, and Z. Huanga, Joining of the C_f/SiC Composites by a One-Step Si Infiltration Reaction Bonding, *Mater. Charact.*, 2019, **155**, p 109799
10. E. Jacques, Y. Le Petitcorps, L. Maillé, C. Lorrette, and L. Chaffron, Joining Silicon Carbide Plates by Titanium, *Powder Metall. Met. Ceram.*, 2014, **52**(9–10), p 606–611
11. Z. He, C. Li, J. Qi, Y. Huang, J. Feng, and J. Cao, Pre-infiltration and Brazing Behaviors of Cf/C Composites with High Temperature Ti-Si Eutectic Alloy, *Carbon*, 2018, **140**, p 57–67
12. B. Riccardi, C.A. Nannetti, J. Woltersdorf, E. Pippel, and T. Petrisor, Joining of SiC Based Ceramics and Composites with Si-16Ti and Si-18Cr Eutectic Alloys, *Int. J. Mater. Prod. Tech.*, 2004, **20**(5–6), p 440–451
13. M. Li, X. Zhou, H. Yang, S. Du, and Q. Huang, The Critical Issues of SiC Materials for Future Nuclear Systems, *Scr. Mater.*, 2018, **143**, p 149–153
14. M. Salvo, P. Lemoine, M. Ferraris, and M. Montorsi, Joining of Carbon-Carbon Composites for Thermonuclear Fusion Applications, *J. Am. Ceram. Soc.*, 1997, **80**(1), p 206–212
15. B. Drevet and N. Eustathopoulos, Wetting of Ceramics by Molten Silicon and Silicon Alloys: A Review, *J. Mater. Sci.*, 2012, **47**, p 8247–8260
16. X. Song, A. Passerone, W. Fu, S. Hu, C. Niu, Y. Zhao, M. Wang, and F. Valenza, Wetting and Spreading Behavior of Sn-Ti Alloys on SiC, *Materialia*, 2018, **3**, p 57–63
17. T.B. Massalski, Binary Alloy Phase Diagrams, *ASM, Met. Park*, 1986, **3**, p 2874
18. P. Dadras, T.T. Ngai, and G.M. Mehrotra, Joining of Carbon-Carbon Composites Using Boron and Titanium Disilicide Interlayers, *J. Am. Ceram. Soc.*, 1997, **80**(1), p 125–132
19. O. Dezellus, S. Jacques, F. Hodaj, and N. Eustathopoulos, Wetting and Infiltration of Carbon by Liquid Silicon, *J. Mater. Sci.*, 2005, **40**, p 2307–2311
20. M. Caccia, S. Amore, D. Giuranno, R. Novakovic, E. Ricci, and J. Narciso, Towards Optimization of SiC/CoSi₂ Composite Material Manufacture via Reactive Infiltration: Wetting Study of Si-Co Alloys on Carbon Materials, *J. Eur. Ceram. Soc.*, 2015, **35**(15), p 4099–4106
21. M. Caccia and J. Narciso, Key Parameters in the Manufacture of SiC-Based Composite Materials by Reactive Infiltration, *Materials*, 2019, **12**, p 2425
22. R. Novakovic, D. Giuranno, M. Caccia, S. Amore, R. Nowak, N. Sobczak, J. Narciso, and E. Ricci, Thermodynamic, Surface and Structural Properties of Liquid Co-Si Alloys, *J. Mol. Liq.*, 2016, **221**, p 346–353
23. S. Amore, D. Giuranno, R. Novakovic, E. Ricci, R. Nowak, and N. Sobczak, Thermodynamic and Surface Properties of Liquid Ge-Si Alloys, *Calphad*, 2014, **44**, p 95–101
24. D. Giuranno, N. Sobczak, G. Bruzda, R. Nowak, W. Polkowski, A. Kudyba, A. Polkowska, and R. Novakovic, Studying the Wettability and Reactivity of Liquid Si-Ti Eutectic Alloy on Glassy Carbon, *J. Mater. Eng. Perform.*, 2019, **28**, p 3460–3467
25. D. Giuranno, N. Sobczak, G. Bruzda, R. Nowak, W. Polkowski, A. Kudyba, A. Polkowska, and R. Novakovic, Wetting and Spreading Behaviors of Liquid Si-Ti Eutectic Alloy in Contact with Glassy Carbon and SiC at $T = 1450$ °C, *Metall. Mat. Trans A*, 2019, **50**(10), p 4814–4826
26. F. Valenza, V. Casalegno, S. Gambaro, M.L. Muolo, A. Passerone, M. Salvo, and M. Ferraris, Surface Engineering of SiCf/SiC Composites by Selective Thermal Removal, *Int. J. Appl. Ceram. Technol.*, 2017, **14**, p 287–294
27. R. Novakovic, E. Ricci, M.L. Muolo, D. Giuranno, and A. Passerone, On the Application of Modelling to Study the Surface and Interfacial Phenomena in Liquid Alloy-Ceramic Substrate Systems, *Intermetallics*, 2003, **11**(11–12), p 1301–1311
28. M. Caccia, D. Giuranno, J.M. Molina, M. Moral, R. Nowak, E. Ricci, N. Sobczak, J. Narciso, and J.F. Sanz, Graphene Translucency and Interfacial Interactions in the Gold/Graphene/SiC System, *J. Phys. Chem. Lett.*, 2018, **9**(14), p 3850–3855
29. E. Ricci, D. Giuranno, and N. Sobczak, Further Development of Testing Procedures for High Temperature Surface Tension Measurements, *J. Mater. Eng. Perform.*, 2013, **22**(11), p 3381–3388
30. J.J. Biernacki and G.P. Wozak, Stoichiometry of the C + SiO₂ Reaction, *J. Am. Ceram. Soc.*, 1989, **72**, p 122–129
31. A.D. Camarano, D. Giuranno, and J. Narciso, New Advanced SiC-Based Composite Materials for Use in Highly Oxidizing Environments: Synthesis of SiC/IrSi₃, *J. Eur. Ceram. Soc.*, 2020, **40**(3), p 603–611

Publisher's Note Springer Nature remains neutral with regard to jurisdictional claims in published maps and institutional affiliations.